Synthesis, Crystal Structure, Electronic Structure, and Magnetic Properties of In_2ThBr_6

Richard Dronskowski

Max-Planck-Institut für Festkörperforschung, Heisenbergstrasse 1, 70 569 Stuttgart, Germany

Received April 6, 1995[⊗]

In_2ThBr_6, a reduced indium bromide containing univalent indium and tetravalent thorium, is synthesized from indium tribromide, thorium tetrabromide, and elemental indium at moderate temperatures. The monoclinic crystal structure, determined via Rietveld refinement of high-precision X-ray powder diffractometer data (a = 879.12(1) pm, b = 1467.00(2) pm, c = 904.64(1) pm, β = 91.153(1)°; $C2/c$; Z = 4), is built up from three-dimensionally interconnected $ThBr_8^{4-}$ bisdisphenoids and $InBr_9^{8-}$ monocapped cubes, the latter polyhedra being significantly distorted. The analysis of the chemical bonding of In_2ThBr_6, as well as the explanation of the novel compound's weak paramagnetic susceptibility (direct van Vleck type), is based on *ab initio* all-electron scalar-relativistic band structure calculations.

Introduction

While the crystal chemistry of the halides of univalent indium may, at first sight, be considered to be analogous to those of potassium and rubidium, a closer look reveals a fundamental difference that originates in the local electronic structure of In^+. The almost doubly filled 5s atomic orbital of univalent indium leads directly to antibonding interactions with halide p functions in the highest occupied bands, thus favoring strongly widened, often distorted, coordination polyhedra which are most evident in the crystal structures of the reduced binary indium bromides.[1]

From the more experimental, synthetic point of view, the same electronic factor is responsible for the fact that all reduced indium bromides exhibit a slight electrophilic tendency, allowing them to react quite easily with other transition metals at moderate temperatures. By the use of this reactivity, a whole new series of ternary compounds is possible, such as the new phase In_2ZrBr_6, which was recently prepared for the first time.[2] Besides two crystallographic phase transitions, In_2ZrBr_6 is characterized by a weak van Vleck-type paramagnetism that could be successfully explained by proposing a hitherto unknown, *indirect* electronic coupling between indium 5s centered frontier bands and empty, fairly localized zirconium 4d crystal orbitals via bridging bromine 4p functions.

Since Zr^{4+} is the largest tetravalent transition metal cation, its replacement against the still somewhat larger Th^{4+} was attempted to yield additional information about the influence of the cationic size on the magnetic mechanism. On the other hand, the mutual interplay of the energetically almost degenerate 6d and 5f atomic orbitals of thorium (compared to zirconium 4d) further introduces another electronic parameter that would surely affect the chemical and physical properties of In_2ThBr_6, making any predictions concerning the structure and magnetic behavior of In_2ThBr_6 admittedly difficult. As an illustrative example, the fore-mentioned 6d/5f competition was recently experimentally manifested in the complex solid state cluster chemistry of thorium.[3−5] In the following, we therefore report on various experimental and theoretical investigations on the new phase In_2ThBr_6.

Experiments and Theory

1. Synthesis. In_2ThBr_6 was synthesized in quantitative yield from a synproportionation reaction of a stoichiometric mixture of $ThBr_4$, $InBr_3$, and elemental In within an evacuated glass ampoule at 450 °C for 5 days. $ThBr_4$ itself was made from the elements[6] while $InBr_3$ was prepared from aqueous solution.[7] Both materials were then purified by repeated sublimations. Indium shots (Alfa, 4N) were used as purchased. The melt was slowly cooled down to 100 °C at a rate of 2 °C/h and then to room temperature at 20 °C/h.

Pure powderous In_2ThBr_6 is almost white, with a slight amberlike tint. The attempt to grow single crystals in the temperature gradient 200/300 °C was almost unsuccessful; the nearly colorless objects that could be obtained may best be described as "sintered powder" judging from their mediocre Laue X-ray patterns, only in some cases indicating the presence of one slightly larger crystalline individual inside the macroscopic object. Even more unfortunately, In_2ThBr_6 is extremely sensitive to air and humidity and must be strictly handled under a protective argon atmosphere.

2. Crystal Structure Analysis. The X-ray powder pattern of In_2ThBr_6, recorded on a powder diffractometer, immediately revealed a low crystal symmetry. Fortunately, powder indexing (ITO-12)[8] went surprisingly straightforward in that 37 reflections between 11.7 and 59.7° in 2θ were indexed, suggesting a monoclinic C-centered unit cell with an extraordinarily high figure-of-merit (119.7), indicating that the cell found had to be correct. Besides that, space groups Cc and $C2/c$ seemed to be plausible.

2.1. Structure Solution. The first structure solution attempt was undertaken from a badly crystallized object of irregular shape mounted on an imaging plate diffractometer. After some effort, both the crystal class and the unit cell dimensions already found from powder were reidentified. Also, despite the object's exceedingly low crystal quality (R_{int} = 0.404, R_σ = 0.284), the course of the systematic absences again indicated space groups Cc and $C2/c$, for which a Patterson map (SHELXS-86)[9] yielded five strong peaks which later proved to be very close to the correct atomic positions.

In an alternative, more direct way, a restricted set of powder diffractometer data between 5 and 80° in 2θ was automatically decomposed, with considerable computational effort, using the ALL-HKL program[10] and a refinable Voigt function,[11] by that extracting 366 unique structure factors. Moreover, this procedure impressively

[⊗] Abstract published in *Advance ACS Abstracts,* August 15, 1995.

(1) Dronskowski, R. *Inorg. Chem.* **1994**, *33*, 6201.
(2) Dronskowski, R. *J. Am. Chem. Soc.* **1995**, *117*, 1991.
(3) Böttcher, F.; Simon, A.; Kremer, R. K.; Buchkremer-Hermanns, H.; Cockcroft, J. K. *Z. Anorg. Allg. Chem.* **1991**, *598*, 25.
(4) Böttcher, F.; Simon, A.; Cockcroft, J. K. *Angew. Chem.* **1991**, *103*, 79; *Angew. Chem., Int. Ed. Engl.* **1991**, *30*, 101.
(5) Braun, T. P.; Simon, A.; Böttcher, F.; Ueno, F. *Angew. Chem.* **1995**, *107*, 647; *Angew. Chem., Int. Ed. Engl.* **1995**, *34*, 567.
(6) Scaife, D. E. *Inorg. Chem.* **1966**, *5*, 162.
(7) Ensslin, F.; Dreyer, H. *Z. Anorg. Allg. Chem.* **1942**, *249*, 119.
(8) Visser, J. W. *J. Appl. Crystallogr.* **1969**, *2*, 89.
(9) Sheldrick, G. M. *Acta Crystallogr.* **1990**, *A46*, 467.
(10) Pawley, G. S. *J. Appl. Crystallogr.* **1981**, *14*, 357.

0020-1669/95/1334-4991$09.00/0

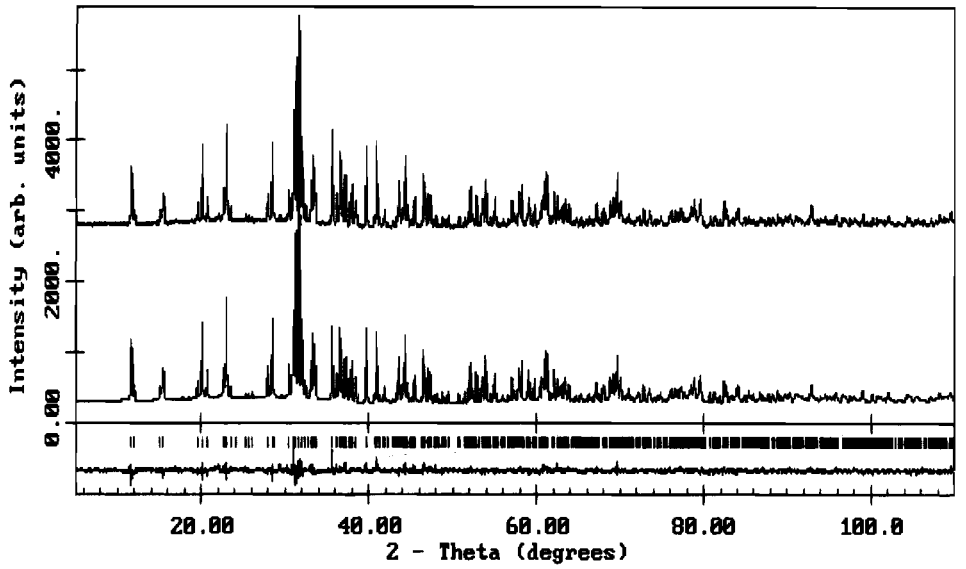

Figure 1. Rietveld refinement of In_2ThBr_6. Depicted are (from top to bottom) measured and fitted diffraction patterns, calculated positions of the Bragg peaks, and the difference between measured and calculated intensities.

Table 1. Crystallographic Data for In_2ThBr_6

formula; molar mass	In_2ThBr_6; 941.10 g/mol
lattice constants	a = 879.12(1) pm, b = 1467.00(2) pm, c = 904.64(1) pm, β = 91.153(1)°
space group; no. of formula units	$C2/c$—C_{2h}^6 (No. 15); 4
X-ray density; $F(000)$	5.359 g/cm^3; 1172
absorption coefficient	95.61 mm^{-1}
sample dimension	0.3 mm glass capillary
instrument	Stoe STADI powder diffractometer, Cu Kα_1 radiation, graphite monochromator, proportional counter
scan type, range, step	2θ, 5° < 2θ < 109.97°, 0.01°
scan speed	25 s/step
temperature	293(1) K
no. of data points, Bragg reflections	10 498, 790
absorption correction	cylindrical correction
structure solution	Patterson map, direct methods
structure refinement	Rietveld least-squares method
profile function	pseudo-Voigt
n_A, n_B mixing parameters	0.84(2), −0.0087(4)
u, v, w half-width parameters	0.070(2), −0.054(2), 0.0212(4)
preferred orientation function	March−Dollase, G = 1.059(2)
asymmetry parameter	0.61(3)
no. of variables, restraints	31, 0
R_p, R_{wp}	0.043, 0.055
$R_{Bragg}(F)$, goodness of fit	0.055, 1.11

confirmed the fore-mentioned space groups *Cc* and *C2/c*. The resolution of the data was good enough to allow direct methods (optimized for powder data) to solve the crystal structure (SIRPOW-92),[12] yielding five heavy atoms that were indeed equivalent to those atoms from the "single-crystal" Patterson map.

2.2. Structure Refinement. The final structure refinement was again based on high-precision powder diffractometer data (Stoe STADI, focusing primary monochromator, transmission technique) between 5.00 and 109.97° in 2θ. In the first stages, the background was manually subtracted by linear interpolation and, afterward, smoothed by linear, nonrecursive filtering in the last three refinement cycles, a filter width of about 1% of the total number of data points having been selected. Using scattering factors for Th^{4+}, In^0, and $Br^{0.13}$ the Rietveld refinement (DBW 9006)[14] in space group *C2/c* converged quickly and confirmed the chemical formula. An alternative refinement in the acentric space group *Cc* led to essentially the same (but less accurate) structure and was discarded. The pseudo-Voigt profile function employed was based on five parameters for the reflection shape, accompanied by one zero-point parameter, one parameter for preferred orientation (March−Dollase function), one asymmetry parameter, one overall scale parameter, four parameters for the lattice constants, thirteen spatial atomic parameters, and five isotropic displacement parameters.

The superb quality of the structure refinement from powder (25-fold overdetermination based on the number of Bragg peaks, R_{wp} = 0.055) is easily perceptible from the tiny standard deviations of all bond lengths (0.1−0.4 pm); in fact, the present refinement shows a higher accuracy than the latest single-crystal refinement of α-$ThBr_4$.[15] However, since it is well-known that Rietveld refinements tend to overestimate the precision of the lattice parameters a little, their refined standard deviations were interpreted quite pessimistically and brought to a round figure.[16]

Table 2. Positional Parameters and Isotropic Displacement Parameters (B_{iso}, Å^2) for In_2ThBr_6 (Standard Deviations in Parentheses)

atom	Wyckoff position	x	y	z	B_{iso}
In	8*f*	0.0132(3)	0.3462(1)	0.0009(3)	4.51(6)
Th	4*e*	0	0.0607(1)	1/4	0.36(2)
Br(1)	8*f*	0.0189(3)	0.1134(2)	0.9418(3)	2.22(7)
Br(2)	8*f*	0.2038(3)	0.2235(2)	0.2683(3)	1.79(7)
Br(3)	8*f*	0.3074(3)	0.0063(2)	0.7354(3)	2.73(8)

An overview of the refinement is given in Figure 1, while all relevant numerical details of the structure determination may be found in Table 1. Positional and isotropic displacement parameters are listed in Table 2. All positions are fully occupied, and the relative sizes of the isotropic displacement parameters match our experiences derived from other reduced phases containing weakly-bonded In^+. The interatomic distances are given in the figure caption of Figure 3.

2.3. Electronic Structure Calculations. The electronic structure calculations of In_2ThBr_6 were based exclusively on *ab initio* all-electron scalar-relativistic techniques such that the most relevant heavy-atom properties of thorium could be taken into account. The analysis of the chemical bonding could then be based on theoretical density-of-states curves and full-potential charge density plots.

The specific method used was the linear muffin-tin orbital (LMTO) theory[17-19] which, in a nutshell, represents a fast, linearized form of the KKR method.[20,21] It accounts for the potential from all the electrons and is applicable to materials composed of atoms from any part of the periodic table. The almost minimal, unfixed LMTO basis sets adjust dynamically to the respective potentials. While the wave functions of the valence electrons are expanded into Hankel envelope functions in the interstitial regions with flat potentials, numerical solutions of the radial Dirac equation are computed in the corelike regions.

The electronic energy was calculated via density-functional theory, replacing the many-particle problem by the self-consistent solution of the Kohn–Sham equations,[22,23] parametrized according to von Barth and Hedin.[24] Diagonalization and integration of the non-spin-polarized, scalar-relativistic Hamiltonian in k space was performed with the help of an improved tetrahedron method[25] using 78 inequivalent k points and 748 different tetrahedra. The basis set of short-ranged[26] atom-centered TB-LMTO's contained s–f valence functions for Th and s–d valence functions for all other atoms. In 5d and Br 5s and 4d orbitals were included using a downfolding technique. Additionally, another 24 "empty spheres" (atomic wave functions without nuclei) per cell were incorporated in order to increase variational freedom and improve packing. Starting from atomic Hartree potentials, we then iterated the structure by use of the atomic-spheres approximation (ASA), employing muffin-tin spheres blown up to overlapping and volume-filling spheres, also including a combined correction term. After self-consistency was attained, charge density plots were generated upon switching to the full-potential LMTO mode, dropping any shape approximations for the potential inside the crystal. The program used was TB-LMTO 4.6,[27] run under LINUX on a 66 MHz Intel 486 processor.

2.4. Magnetic Measurements. The susceptibility measurements of In_2ThBr_6 were performed on a powderous 167 mg sample with the help of a Quantum Design MPMS 5.5 SQUID susceptometer within a temperature range of 2–300 K at a field strength of 1 T. Because of its radioactivity and toxicity, the sample was double-sealed first into a gelatine capsule and second into a quartz glass capillary; the two containers were then evacuated. While the magnetic signal of the quartz glass capillary was zero because of the chosen experimental setup, the correction for the gelatine capsule was based on its mass and mass susceptibility. The diamagnetic influence of the atomic core shells on the molar susceptibilities was taken into account using tabulated values for Th^{4+} and Br^-.[28] The interpolated value for In^+ (-23×10^{-6} cm^3/mol) was the same as in the investigation on In_2ZrBr_6.[2]

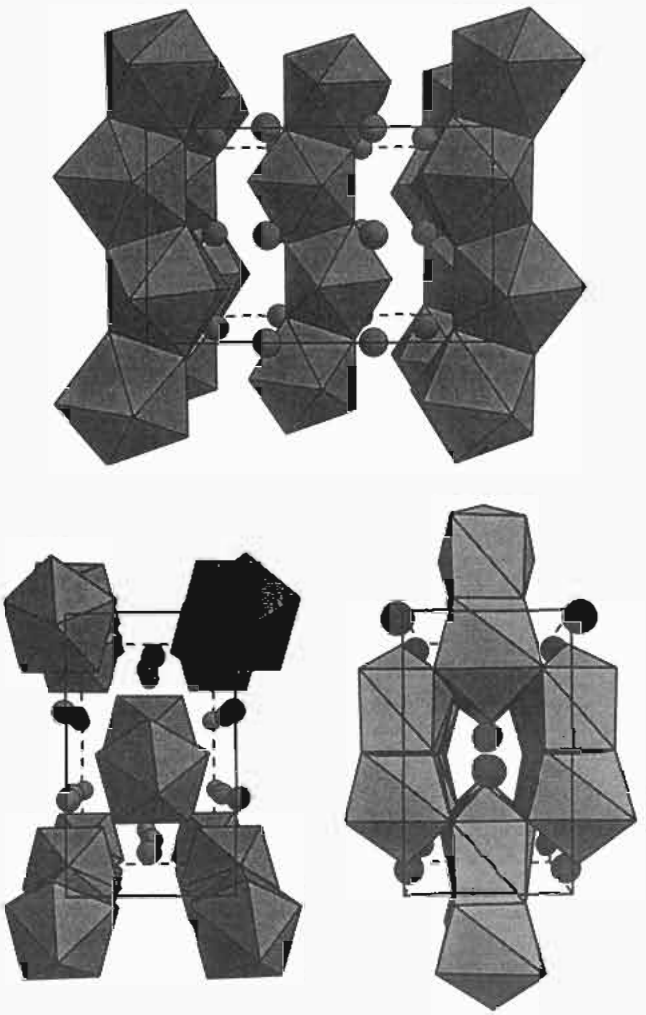

Figure 2. (a) Top: Polyhedral view of the In_2ThBr_6 crystal structure along the a axis, showing the positions of the $ThBr_8^{4-}$ triangulated dodecahedra and those of the univalent indium cations. (b) Bottom: left, same as before but along the c axis; right, same orientation but showing the positions of the interconnected $InBr_9^{8-}$ polyhedra and those of the tetravalent thorium cations.

Results and Discussion

The crystal structure of In_2ThBr_6, of which a perspective polyhedral view along a is presented in Figure 2a, is characterized by $ThBr_8^{4-}$ triangulated dodecahedra that share opposite edges, forming one-dimensional ribbons that run along the c axis in 0, 0, c and in $^1/_2$, $^1/_2$, c. Univalent indium cations occupy the otherwise empty channels between those ribbons.

This *Aufbau* principle may be equally well understood from a corresponding view along the c axis (Figure 2b, left), in which the ribbons then point directly in the viewer's direction. Alternatively, one may emphasize the In^+/Br^- network (Figure 2b, right), which is built up from both face- and corner-sharing, admittedly distorted, monocapped cubes of coordinating Br^- around In^+ ions. In this complementary description focusing on $InBr_9^{8-}$ polyhedra, thorium cations lie in the remaining structural channellike voids.

A closer look at the specific coordination of Th^{4+} is given in Figure 3a. Inside the triangulated dodecahedron (or bisdisphenoid), the eight $Th^{4+}-Br^-$ bond distances range from 288 to 309 pm and may be directly compared with those of the 8-fold coordination inside α-$ThBr_4$ (room-temperature phase), which

(11) David, W. I. F.; Matthewman, J. C. *J. Appl. Crystallogr.* **1985**, *18*, 461.
(12) Altomare, A.; Cascarano, G.; Giacovazzo, C.; Guagliardi, A.; Burla, M. C.; Polidori, G.; Camalli, M. *J. Appl. Crystallogr.* **1994**, *27*, 435.
(13) *International Tables for X-Ray Crystallography*; Ibers, J. A., Hamilton, W. C., Eds.; The Kynoch Press: Birmingham, U.K., 1974; Vol. IV. The scattering factor of Th^{4+} gave a slightly better fit to the experimental data than the one of neutral Th.
(14) Young, R. A. *Program for Rietveld Analysis of X-Ray and Neutron Powder Diffraction Patterns*: *DBW 9006*, rel. 8.4.91; School of Physics, Georgia Institute of Technology: Atlanta, GA 30322.
(15) Mason, J. T.; Jha, M. C.; Bailey, D. M.; Chiotti, P. *J. Less-Common Met.* **1974**, *35*, 331.
(16) Bérar, J.-F.; Lelann, P. *J. Appl. Crystallogr.* **1991**, *24*, 1.
(17) Andersen, O. K. *Phys. Rev. B* **1975**, *12*, 3060.
(18) Skriver, H. L. *The LMTO Method*; Springer: Berlin, Heidelberg, New York, 1984.
(19) Andersen, O. K.; Jepsen, O.; Sob, M. In *Electronic Band Structure and its Applications*; Yussouff, M., Ed.; Springer: Berlin, Heidelberg, New York, 1986.
(20) Korringa, J. *Physica* **1947**, *13*, 392.
(21) Kohn, W.; Rostoker, N. *Phys. Rev.* **1954**, *94*, 1111.
(22) Hohenberg, P.; Kohn, W. *Phys. Rev. B* **1964**, *136*, 864.
(23) Kohn, W.; Sham, L. J. *Phys. Rev. A* **1965**, *140*, 1133.
(24) von Barth, U.; Hedin, L. *J. Phys. C* **1972**, *5*, 1629.
(25) Blöchl, P. E.; Jepsen, O.; Andersen, O. K. *Phys. Rev. B* **1994**, *49*, 16223.
(26) Andersen, O. K.; Jepsen, O. *Phys. Rev. Lett.* **1984**, *53*, 2571.

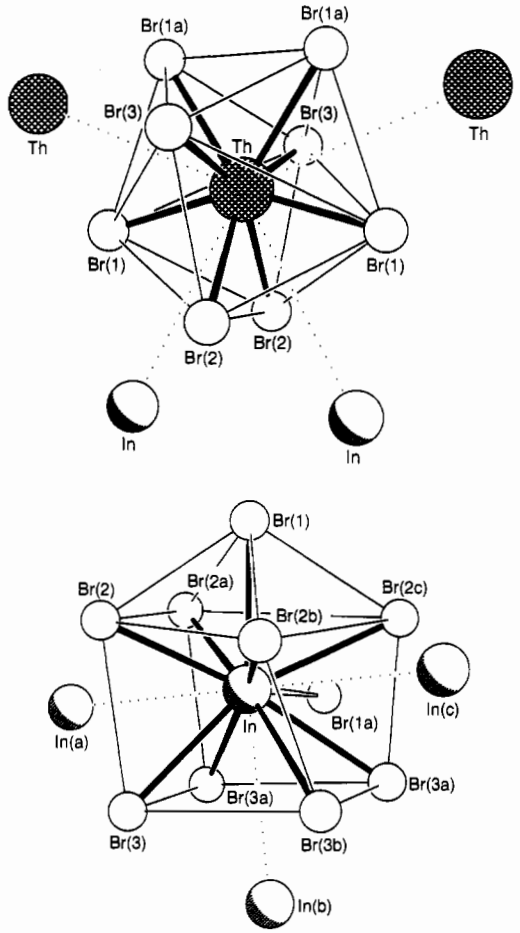

Figure 3. (a) Top: Coordination of tetravalent thorium (large crosshatched circle) by bromine counterions (small open circles) and univalent indium cations (medium-sized shaded circles). The edges of the triangulated dodecahedron are emphasized by thin lines. The $Th^{4+}-Br^-$ bond lengths (pm) are 288.1(3) to Br(3), 290.1(3) to Br(1), 298.8(3) to Br(2), and 309.0(3) to Br(1a). The shortest $Th^{4+}-In^+$ and $Th^{4+}-Th^{4+}$ distances are 475.9(2) and 486.1(1) pm. (b) Bottom: Same as before but showing the coordination of univalent indium. The interatomic distances (pm) of In^+ are 337.6(4) to Br(2), 342.6(4) to Br(2a), 345.7(3) to Br(1), 355.1(4) to Br(3), 355.5(4) to Br(2b), 356.5(4) to Br(3a), 366.2(4) to Br(2c), 379.3(4) to Br(3b), 417.8(4) to Br(1a), 451.8(4) to In(a), 451.8(2) to In(b), and 454.1(4) to In(c).

range from 291 to 302 pm.[15] If one fits the latter bond lengths to the bond length−bond strength formula of Brown and Altermatt,[29] a standard parameter for tetravalent thorium bonded to Br^- of $r_0 = 270.4$ pm results which, applied to the $Th^{4+}-Br^-$ bond lengths inside In_2ThBr_6, yields a formal valence of +4.05 for Th^{4+} inside the new compound. The four shortest thorium−metal distances (Figure 3a), on the other hand, are far too long to allow for any covalent interaction besides some electrostatic repulsion.

Figure 3b shows the coordination polyhedron around the univalent indium cation. The distorted polyhedral geometry may be regarded as the typical In^+ "fingerprint", simply reflecting the unusual local electronic structure of this ion with predominantly antibonding combinations acting in the highest occupied bands. While In^+-Br^- distances of up to 450 pm have to be taken into account to give a reliable description of all covalent interactions,[1] it is evident that nine out of the ten nearest bonds

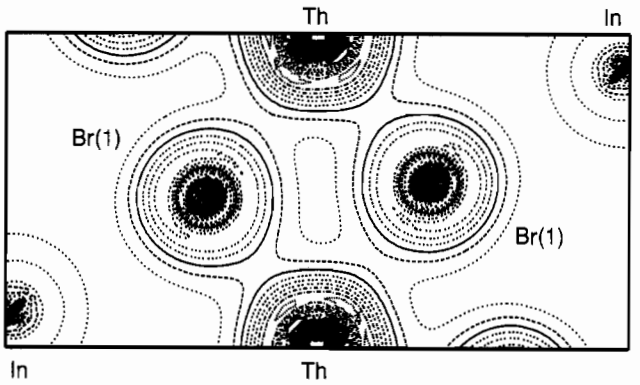

Figure 4. Chemical bonding from an *ab initio* charge density inside In_2ThBr_6. The observable quantity in the approximate plane (Th−Br(1) = 290.1, 309.0 pm; In−Br(1) = 345.7 pm) is divided into 20 equidistant contours between 0 and 0.35 e/a_0^3 where a_0 is the Bohr radius of about 52.9 pm. The outermost "ring" around In^+ is 0.0175 e/a_0^3.

between 338 and 379 pm build up the distorted monocapped "cube" previously mentioned, augmented by one additional In^+-Br^- combination of 418 pm, which caps another neighboring "quadratic" face of the "cube". On the basis of the recently evaluated optimum bond length−bond strength parameter (r_0 = 266.7 pm) for the In^+-Br^- pair,[1] the 9+1 coordination leads to an empirical valence of +0.89 for In^+, a reasonable value. Besides that, the three nearest indium cations have nonbonding distances of little more than 450 pm.

The different characters of chemical bondings inside the coordination polyhedra of Th^{4+} and In^+ can be nicely visualized from an *ab initio* charge density inside the (approximate) plane containing both thorium and indium as well as the Br(1) atom, depicted in Figure 4. Besides the underlying Coulomb interaction, there is a significant amount of covalency in the $Th^{4+}-Br^-$ bond present, clearly resulting from the residual electron density between these two atoms. Because of the both bonding and antibonding covalent interactions in the In^+-Br^- bond, however, the net amount of covalent bond strength is small here, as is the electron density between In^+ and Br^-. As a side effect of this, the resulting crystal potential acting on In^+ is very soft and is observable both theoretically, from the slow decay of the charge density around In^+, and experimentally, from the enlarged isotropic displacement parameter of the crystal structure analysis (Table 2). Indeed, second-order Jahn−Teller instabilities originating from such soft crystal potentials around In^+ were recently brought to attention.[30,31]

Coming now to the physical properties of In_2ThBr_6, Figure 5a shows its magnetic behavior. Neglecting the increase in susceptibility below 50 K, which is due to traces of paramagnetic contaminations that can never be excluded, the thorium compound exhibits a small but *positive* signal up to room temperature, very similar to the case of In_2ZrBr_6.[2] Such weakly paramagnetic character is still easier to recognize from Figure 5b, in which the compound's molar susceptibility is given as a function of the reciprocal temperature. A linear extrapolation to infinite temperatures then evidences a residual paramagnetic susceptibility of about $1.6(1) \times 10^{-4}$ cm^3/mol that needs to be theoretically explained.

To do so, the *ab initio* valence density-of-states (DOS) curve of In_2ThBr_6 is presented in Figure 6, with the local indium 5s contributions emphasized in black. The latter atomic functions are mixing exclusively into the energy region between roughly −9 eV and the Fermi energy (about −5 eV, dashed line), *i.e.*

(27) Program TB-LMTO 4.6 by G. Krier, O. Jepsen, A. Burkhardt, and O. K. Andersen.
(28) Selwood, P. W. *Magnetochemistry*, 2nd ed.; Interscience Publishers: New York, 1956.
(29) Brown, I. D.; Altermatt, D. *Acta Crystallogr.* **1985**, *B41*, 244.
(30) Dronskowski, R. *Angew. Chem.* **1995**, *107*, 1230; *Angew. Chem., Int. Ed. Engl.* **1995**, *34*, 1126.
(31) Dronskowski, R. *Chem. Eur. J.* **1995**, *1*, 118.

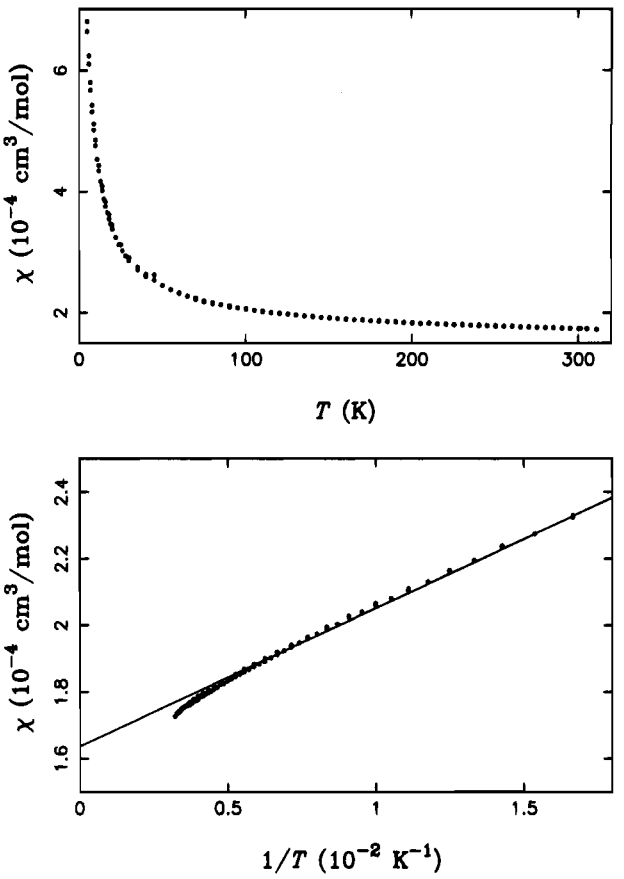

Figure 5. (a) Top: Molar susceptibility as a function of the temperature for In_2ThBr_6 at a field strength of $H = 1$ T. (b) Bottom: Same as before but as a function of the reciprocal temperature. The interpolated line corresponds to a linear fit of the high-temperature data.

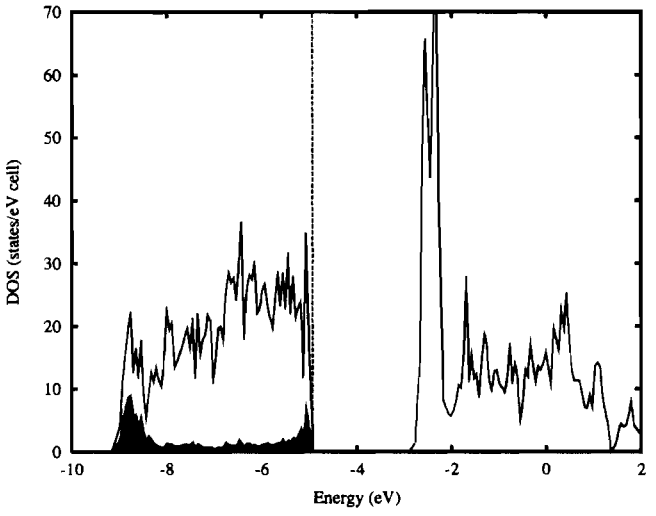

Figure 6. *Ab initio* density-of-states (DOS) for In_2ThBr_6 with the local indium 5s projections emphasized in black. The double peak around −2.5 eV exhibits almost exclusively thorium 5f character.

the occupied valence bands that are strongly Br 4p dominated. Besides that, one also finds additional Th 7s (weak) and Th 6d (stronger) contributions here. In comparison, the virtual bands fall into two different categories. While the strongly dispersed region above −2 eV arises mainly from Th 6d and the highly diffuse In 5p functions, moderated by a little Br 4p mixing, the well-localized virtual double peak at −2.5 eV carries practically pure Th 5f character.

Thus, any *indirect, through-bond* kind of paramagnetism of van Vleck type must be immediately rejected for In_2ThBr_6. In contrast to the situation in In_2ZrBr_6, there is no such mixing determinable between the In 5s functions of the diamagnetic ground state and the unoccupied bands (Th 5f-centered) since the latter exhibit no (black) indium 5s contribution. While such coupling via mediating Br atoms was possible for In_2ZrBr_6 because of the diffuse nature of the "acceptor" zirconium 4d levels, the thorium 5f functions are possibly too strongly contracted to interact in an analogous way.

On the contrary, the band structure calculations suggest that the observed residual paramagnetic signal arises *directly* from the thorium atom itself, just as in the spirit of a standard van Vleck-type mechanism. Consequently, there must be available thorium levels *below* the virtual 5f bands out of which the applied magnetic field can introduce electronic excitations. In this respect, one needs to know the positions of the self-consistent band centers, reflecting the *average* energies of the electrons with different angular momentums, similar to those H_{ii} values of semiempirical extended Hückel theory. As it turns out, these band center positions of the 7s, 6d, and 5f thorium functions arrive at −4.93, −1.46, and −1.68 eV, indicating that mostly 7s−5f and, to a lesser extent, 7s−6d van Vleck mixing is truly to be expected. Such an on-site atomic process, however, could be excluded for the case of Zr^{4+} in In_2ZrBr_6 where the 4d band position happened to be the *lowest* one of the zirconium atom.

It is disappointing that corresponding fundamental magnetic investigations are missing for the simple thorium halides up to now. However, it appears that Tilk and Klemm have reported a similar paramagnetic effect for thorium dioxide, ThO_2, and other closed-shell phases.[32] Their qualitative proposal of the mechanism relies on a perturbation effect affecting the high-frequency precession of Th^{4+} within the magnetic field. This description is simply the old quantum mechanics' analogue of the direct van Vleck angular momentum operator, promoting an electron from the ground state (7s) into some excited state (5f, 6d) by the outer magnetic field.

Acknowledgment. It is a pleasure to thank Dr. Thomas P. Braun for a generous gift of pure thorium tetrabromide and Dr. Rainer Pöttgen for his help in operating the imaging plate diffractometer. Also, I am indebted to Drs. Angela Altomare and Gianluca Cascarano (Bari, Italy) for providing source code copies of the magnificent ALLHKL and SIRPOW programs as well as to Drs. Antonella Guagliardi and Anna G. Moliterni for friendly Internet assistance on how to use them. Additional thanks are directed to Mrs. Eva Brücher and Dr. Reinhard K. Kremer for performing the magnetic susceptibility measurement. Finally, I would like to acknowledge the steady support by Prof. Dr. Arndt Simon and additional financial help by the Fonds der Chemischen Industrie (Frankfurt, Germany).

IC950402L

(32) Tilk, W.; Klemm, W. *Z. Anorg. Chem.* **1939**, *240*, 355.